

A Seismo-Geodetic Amphibious Network in the Guerrero Seismic Gap, Mexico.

Víctor M. Cruz-Atienza*, Yoshihiro Ito, Vladimir Kostoglodov, Vala Hjörleifsdóttir, Arturo Iglesias, Josué Tago, Marco Calò, Jorge Real, Allen Husker, Satoshi Ide, Takuya Nishimura, Masanao Shinohara, Carlos Mortera-Gutierrez and Soliman García.

*Corresponding author: cruz@geofisica.unam.mx

Submitted to the Seismological Research Letters

September 7, 2017

Abstract

The historical record of large subduction earthquakes in Guerrero, Mexico, reveals the existence of a ~230 km length segment below the coast where no major rupture has occurred in the last 60 years. A future megathrust earthquake ($M_w \sim 8.2$) in this seismic gap represents the largest natural hazard to Mexico City, where more than 20 million people live, and to several large towns/cities along the Mexican Pacific coast due to the expected ground motion and tsunamis. Reliable quantification of such hazards is urgently needed for the risk mitigation by means of state-of-the-art observations allowing robust assessments of the regional seismic potential. In this manuscript, we introduce the first seismo-geodetic amphibious network deployed in Mexican and Central American soils that will provide the opportunity to achieve these goals in the near future. This network along with the associated scientific work is the result of collaborative efforts between scientists from Mexico and Japan. The observational network provided by this collaboration consists of 14 broadband seismometers, 7 ocean bottom seismometers, 33 GPS stations, 7 ocean bottom pressure gages and 2 GPS-Acoustic sites. These instruments complement three permanent

networks covering the seismic gap and its surroundings (i.e. a region of ~400 km along the coast and ~250 km in the trench-perpendicular direction), which make the target area very well instrumented with a total of 31 seismometers, 48 geodetic stations and 83 accelerometers. Resolution analyses for future tomographic imaging of the earth structure and slow slip transients in the plate interface are presented considering the amphibian network configuration. Synthetic inversion tests from seismic and geodetic data reveal the benefits of the new observational network that should lead to unprecedented high-resolution results along the subduction margin up to the Middle American trench. These studies are expected to improve our understanding of the subduction process in the region and to produce better assessments of the associated earthquake and tsunami hazards.

1. Introduction

Three major subduction thrust earthquakes since 2004 with $M_w \geq 8.8$ (Lay et al., 2012) and the associated humanitarian tragedies around the world, primarily due to the tsunamis generated, have raised fundamental questions in the communities devoted to understanding hazard assessment and physics of earthquakes. Among the lessons learned from these events includes accepting the possibility of future ruptures much larger than those documented in the historical records of any subduction zone. Disaster risk assessment and prevention from this kind of scenarios in the future requires new and more sophisticated observational facilities aiming to monitor any tectonic manifestation related to the seismic cycle. Data recorded in the vicinity of the seismogenic faults may lead to unprecedented quantification of the earthquake potential and constraints for physics-based models leading to more reliable hazard assessments.

As revealed by past events, seismicity along the Pacific coast of Mexico produced by the interaction of the subducting Cocos plate and the overriding North American plate represents a high risk of disaster in the near future related to megathrust earthquakes and tsunamis (e.g. 1985 $M_w 8.0$: Anderson et al., 1986 and 1787 $M \sim 8.6$: Suárez and Albin, 2009). In particular, a ~ 230 km long segment of the Mexican subduction zone offshore and below the coast of state of Guerrero has not broken in a significant rupture ($M \geq 7.0$) in at least 60 years. Recent earthquakes that occurred in April (Papanao, $M_w 7.3$) and May ($M_w 6.5$ and $M_w 6.1$) 2014 on the Costa Grande of the state (west from Acapulco, Figure 2) are a reminder of what has been preparing for more than 106 years in that 130 km long segment of the seismic gap, between Acapulco and Papanao (Figure 1). The main event

initiated outside the gap and halted right in its western edge, while the May events broke within the gap (UNAM Seismology Group, 2015). East from Acapulco (Figure 2), below (and offshore) the Costa Chica of the state, another ~100 km long segment extends where the last major earthquake occurred in 1957 (Singh et al., 1982; Duke and David, 1995). Considering that (1) the return period by segment for major ($M \geq 7.0$) subduction earthquakes in Mexico ranges between 30 and 60 years (Singh et al., 1981), and that (2) only between 1899 and 1911 a sequence of seven large and very large earthquakes occurred in the Costa Grande region (all of them with a magnitude larger than or equal to 7, and a maximum magnitude of 7.9) (UNAM Seismology Group, 2015), the specialists believe that a $M_w \approx 8.2$ earthquake with ~230 km long rupture in the extended Guerrero seismic gap (GGap) (Figures 2 and 3) is a severe but plausible scenario for the near future. Such a rupture could produce spectral accelerations in Mexico City two to three times larger than those experienced during the devastating $M_w 8.0$ Michoacán earthquake of 1985 (Kanamori et al., 1993), which killed ~10,000 people in the capital of Mexico where more than 22 million people live today.

Detailed investigations of the three worldwide megathrust earthquakes referred to above have revealed that most of the seismic moment in all cases was released in the offshore part of the plate interface, close to the trench, raising fundamental questions about the nature of the rupture process in subduction zones (see Lay et al., 2012 and reference therein). We know little about the plate-interface processes taking place between the middle-American trench and the coast of Mexico, where the expected large rupture in Guerrero may produce a disastrous tsunami similar to the one that occurred in 1787 along the coast of Oaxaca due to a $M \sim 8.6$ event (Núñez-Cornú et al., 2008; Suárez and Albin, 2009). In Japan and Chile,

for example, offshore slow slip transients have occurred prior to major events (Kato et al., 2012, Ito et al., 2013, Ruiz et al., 2014). The same could happen with the occurrence of tectonic tremor and very low frequency earthquakes (Yamashita et al., 2015; Ito et al., 2015). Thus, slow earthquakes seem to significantly affect the strain accumulation in the seismogenic zone. In the state of Guerrero, long-term slow slip events (SSE) occur approximately every 3.5 years (Cotte et al., 2009) and represent the largest documented aseismic events in the world, with equivalent moment magnitude up to 7.6 (Kostoglodov et al., 2003). Estimates of the seismic coupling in the plate interface suggest that the long-term strain rate accumulation in the Costa Grande segment of the GGap is 75% lower than in the adjacent regions (e.g. the Costa Chica) (Radiguet et al., 2012). Remarkably, the stress perturbation induced by these transients could also lead to the rupture of dynamically mature asperities, as suggested during the Mw7.3 Papanaoa earthquake of April 2014 (Radiguet et al., 2016), whose rupture began during the development of a SSE in the region (UNAM Seismology Group, 2015). Tectonic tremor, low frequency and very low-frequency earthquakes have also been observed in Guerrero close to the plate interface at 40-45 km depth during the occurrence of SSEs (Payero et al., 2008; Kostoglodov et al., 2010; Husker et al., 2012; Cruz-Atienza et al., 2015; Frank et al., 2014; Maury et al., 2016), suggesting that such phenomena are causally related (Villafuerte and Cruz-Atienza, 2017) as suggested for other subduction zones (e.g. Bartlow et al., 2011; Hirose and Obara, 2010).

Understanding this phenomenology, which seems to be present in different subduction zones, results of critical importance to produce reliable hazard assessments for future earthquakes and tsunamis and thus, to mitigate the associated risk. Achieving this in Guerrero requires addressing fundamental questions such as: how the long-term seismic

coupling evolves with time from the trench up to 40 km depth? Do SSEs, tectonic tremor and small (e.g. repeating) earthquakes occur near the trench? How do they behave? How far the long-term SSEs penetrate into the seismogenic zone of the GGap? What are the mechanical properties of the plate interface in the shallow transition zone? Are there pressurized fluids in it? What are the elastic properties and geometry of the subducting Cocos plate? What is the probability of a next megathrust event in the GGap? What could be its maximum slip near the trench and how large would be the associated tsunami? Robust answers to these questions are only possible using data from a seismo-geodetic network overlying the plate interface from the trench (offshore) to inland regions far enough from the coast. This is, by means of seismic and geodetic stations encompassing the seismogenic zone and both the updip and downdip transition zones of the plate interface.

Physics-based earthquake and tsunami scenarios in the GGap constrained by state-of-the-art observations both, onshore and offshore, are thus urgently needed for disasters mitigation caused by future megathrust earthquakes in the Pacific coast of Mexico. To achieve this goal, we, Mexican and Japanese scientists, are developing a seismo-geodetic amphibious network in the region. The network is composed of seismic and geodetic instruments installed offshore and onshore (Figures 2 and 3), as a part of the 2016-2021 international collaborative research project “Hazard Assessment of Large Earthquakes and Tsunamis in the Mexican Pacific Coast for Disaster Mitigation” funded by the Japanese and Mexican governments through different agencies and institutions. The installation of the network will be completed in November 2017. Results from this collaboration should significantly contribute to the risk mitigation in Mexico, and to the identification of similarities (and differences) between the subduction zones of Japan and Mexico, leading to a better

understanding of the physical mechanisms of megathrust earthquakes and tsunamis in subduction margins.

2. Seismo-Geodetic Amphibious Network

Our observational network consists of seismometers and high-resolution geodetic instruments that are being deployed both offshore and onshore around the GGap. The set of seismological stations consists of 14 broadband seismometers (red and purple triangles in Figure 2) and 7 ocean bottom seismometers (OBSs) (pink triangles in Figure 2). There are three different types of geodetic stations. Onshore, the network consists of 33 GPS stations (red, blue and black circles in Figure 3), while offshore it consists of 7 ocean bottom pressure gages (OBPs, yellow triangles in Figure 3) and 2 GPS-Acoustic sites (pink circles in Figure 3). It is worth mentioning that, to our knowledge, this is the first deployment of OBP and GPS-A stations in Mexico and Central America. Each GPS-A site is composed of three ocean bottom transponders making a triangle, as show in Figure 4, where we present an overview of the whole submarine network. To perform GPS-Acoustic measurements we have acquired an autonomous Wave Glider equipped with cutting-edge instrumentation composed of two differential GPS antennas, an optical fiber gyroscope, an acoustic transducer, a control unit and solar panels, based on a design by the University of Singapore (Sylvain Barbot, personal communication) and Seatronics Co. Specifications of the network instruments are given in Table 1. Deployment and operation of the offshore instruments are being conducted using the research vessel “El Puma” of the National Autonomous University of Mexico (UNAM).

Our observational network in Guerrero is complemented by three permanent networks belonging to UNAM and the “Centro de Instrumentación y Registro Sísmico” (CIRES). From UNAM, one of them belongs to the Servicio Sismológico Nacional (SSN) and consists of 10 observatories, each equipped with a Trimble GPS station, a STS-2 broadband seismometer and a FBA-23 accelerometer (black triangles and circles, correspondingly, in Figures 2 and 3), and the other belongs to the Institute of Engineering, with 35 Kinematics FBA-23 accelerometers (green squares in Figure 2). From CIRES, the infrastructure consists of 42 strong-motion 23-bit stations (yellow circles in Figure 2). In total, the GGap and nearby regions (i.e. a region of ~400 km along the coast and ~250 km in the trench-perpendicular direction) are instrumented with 31 seismometers, 48 geodetic stations and 83 accelerometers. 66% (i.e. 14 instruments) of the seismic stations and 45% (i.e. 19 instruments) of the geodetic stations were provided by the Japanese government and, the rest, by the Mexican government. It is worth mentioning that the anchors of 7 OBPs, digitizers from 7 broadband seismometers, GPS electrical components and the installation infrastructure for all onshore sites were also provided by the Mexican government, so the percentages are only indicative.

Seismo-geodetic amphibious networks have only been deployed recently in few region of the globe such as Japan, New Zealand, Turkey, Chile and USA, producing extraordinary observations leading to a much deeper understanding of the plate interface processes (e.g., Yamashita et al., 2015; Wallace et al., 2016; Toomey et al., 2014). As we shall discuss in the next section, our network design responds to the current knowledge we have of the seismotectonic activity in the GGap and surrounding regions, and represents the best achievable compromise between resolution of the future scientific studies and practical

constraints imposed by inaccessible regions. The network will be completely installed by November 2017, a few months before the initiation of the incoming long-term SSE in Guerrero, which is expected to start in the first half of 2018. Among the scientific goals we plan to achieve in the framework of our Mexico-Japan collaboration, that involves about 73 researchers and 27 students from both countries (see Figure 5), are the detection of any aseismic transient and/or secular deformation processes in the GGap, as well as slow, repeating, tsunami and/or conventional earthquakes. From this data, we will perform different seismotectonic studies by analyzing the causative sources, determine the evolution of the seismic coupling as well as the plate interface kinematics responsible of the aseismic transients. In order to determine the crustal structure, we will generate tomographic images using different methods based on double-difference arrival times, regional events and correlation of seismic noise. We will also look for temporal variations of the crustal properties from noise correlations and perform receiver functions analysis. In the case a large rupture takes place, we will image the rupture kinematic process from local strong motion records, teleseismic waves and the static strain field.

3. Resolvability of the Observations

Although the planned work with data from the network is diverse, in this section we present resolution tests for two methodological strategies that are essential to achieve the final goals of the international collaboration. Results from the tests helped us to decide the best locations for the seismic and geodetic sites of the network to maximize the resolvability of both, tomographic and SSE/Coupling imaging. The tests also give us an idea of the characteristic lengths that should be resolved once the data is available.

3.1. Crustal Tomography Resolution

Two tomographic methods will be used to study the continental and oceanic crustal structures from the trench to inland regions of Guerrero. Method 1 is based on double differences of relative and absolute arrival times from passive sources, and Method 2 on dispersion curves determined from the correlation of ambient noise and regional earthquakes.

Method 1: High-resolution wave-velocity models will be obtained using earthquake tomography based on the Double Difference method (Zhang and Thurber, 2003). The algorithm determines 3D velocity models of V_p and V_s jointly, combining the absolute and relative event locations. This approach has the advantage of integrating relative arrival times between pairs of events with error estimates along with absolute arrival times, thereby retaining valuable information often dismissed when only adjusted picks are considered. The final models will be refined by applying the Weighted Average Model method (WAM, Calò et al., 2012, 2013), which is a post-processing technique useful for any tomographic inversion method to overcome some limitations of the velocity models yielded by standard tomographic codes. The post-processing method is based on sampling models compatible with data sets using different input parameters. New and more reliable models are then achieved by means of weighting functions based on the ray density (Derivative Weight Sum, DWS, Toomey and Foulger, 1989).

In order to assess the minimum resolution lengths of the tomographic model we set up a checkerboard test using a plausible earthquakes distribution expected to be recorded in the network during the remaining three years of the project. We used the catalogue of events reported by the SSN since 2000 assuming that the events rate and locations will not significantly change in the next few years. We considered only events with $M > 3.9$ and declustered the catalogue to remove seismic sequences leading to anomalous earthquake concentrations. Then we randomly selected the hypocenters to obtain a representative distribution of the foci with 442 events in a three-year lag time (Figure 6). For the test we assumed that at least 80% of the seismic stations would record the events. We considered 29 stations, from which the international project supplied 21 and the rest belong to the SSN. To make even more conservative our resolution tests, we did not to include the strong motion stations from the Institute of Engineering and the CIRES-SASMEX (green and yellow symbols in Figure 2).

The checkerboard model is characterized by alternating positive and negative velocity changes of ± 5 percent with respect to the initial 1D velocity model. Each patch has size of $20 \times 20 \times 10 \text{ km}^3$ in the X, Y and Z direction, respectively. This model was then used to calculate synthetic travel times using the selected earthquakes configuration and stations, assumed to be representative of the future real inversion. Possible travel time errors were integrated by adding Gaussian distributed noise with a standard deviation of 0.02 and 0.04 s to the P and S travel times, respectively, which corresponds to the largest expected picking error for local/regional datasets digitalized at 100 sps (Chiarabba and Moretti, 2006). Figure 6 shows the resulting model from the inversion, where we conclude that the crustal and also the upper mantle structures are well resolved in a large region surrounding the GGap at

least for velocity anomalies with characteristic lengths similar to the dimensions of the checkerboard patches tested here (20 km horizontally and 10 km vertically).

Method 2: Tomographic images from surface waves analysis will be generated using dispersion curves obtained from noise cross correlations of pairs of stations. To obtain dispersion curves we will follow the “standard” procedure proposed by Bensen (2007). Data from pairs of inland broadband stations (BB-BB) will allow to obtain dispersion curves from ~1 to 50 s depending on the inter-station distances.

Dispersion curves will also be computed for pairs of stations offshore (OBS-OBS) and combinations onshore-offshore sites (BB-OBS) that are expected to have a limited bandwidth between ~1 and ~10 s. Moreover, we also plan to compute dispersion curves for local and regional earthquakes recorded in the network. This mixed data set not only will contribute to improving the resolution of tomographic images, but also will allow having tomographic images for other periods (>10 s). Individual dispersion curves for each pair of station-station and/or earthquake-station will be inverted in a tomographic sense using the “Fast Marching Method” developed by Rawlisson and Sambridge (2005). See Iglesias et al. (2010) and Spica et al. (2014) for details.

To assess the possible resolution of tomographic images considering only noise correlation between pairs of stations close to the coast, we performed a checkerboard test assuming that it will be possible to obtain velocity group measurements for some period between all stations. The study area was subdivided into 20 x 20 cells of 0.1° (~11 km). For the checkerboard test, cells are set with alternating positive and negative velocity changes of ± 8

% with respect to a reference initial homogeneous model (2.6 km/s). Figure 7 shows the results from the synthetic inversion using the checkerboard model. The inversion scheme recovers, reasonable well, the target configuration for the area surrounded by the stations up to distances smaller than 5 km from the trench (not shown).

3.2. Slow Slip and Seismic Coupling Resolution

The evolution of both slow slip transients and the seismic coupling in Guerrero can be inferred from observations recorded in our geodetic amphibious network. The slip inversion will be performed in a constrained optimization framework using the adjoint method for a simple and efficient gradient evaluation (Tarantola, 1984; Plessix, 2006). The observations will correspond to displacement time-series recorded at onshore GPS stations, and offshore OBP and GPS-A sites. From a linear formulation of the elastostatic problem and a quadratic cost function given by the square difference of the observed and synthetic displacements, the resulting optimization problem is convex and has unique solution. Two of the most valuable advantages of this strategy are (1) that the slip function in the plate interface is not parameterized, and (2) that it is possible to estimate, a posteriori, the formal uncertainty of the model parameters. The lack of complete fault illumination, the noise in the data and the model uncertainties hinder the slip or coupling inversions. However, regularization and prior model terms can be integrated in the problem formulation for overcoming these problems to some extent. Although this is an ongoing work in the framework of our collaborative project, this new inversion method has already been validated for a homogeneous full space. Steps leading to a more realistic model configuration (e.g. including a heterogeneous halfspace) are being undertaken and only

require the computation of the elastostatic Somigliana tensor in the desired earth model (Udías et al, 2014).

In order to have an insight of the inverse-model resolution given the actual configuration of the geodetic network and the 3D geometry of the plate interface in Guerrero, we performed a series of synthetic inversion tests. For all tests, the stations are located in the same horizontal plane above the interface, which is discretized by subfaults with horizontal square projections of 5 km per side. Figures 8a-c show the results for checkerboard inversion tests considering different problem setups where only the along-dip slip component was inverted. Although smoother, results that also include the along-strike component are very similar (not shown). The checkerboard is composed of squares with 80 km per side, with slip of either 0 or 30 cm. Figures 8a and 8b show the inversion results for a station array with regular spacing and the actual stations network, respectively, considering a horizontal plate interface 40 km below the stations. For most of sites offshore, we only inverted the vertical displacement component, which is expected to be recorded by the OBPs, while for the two GPS-A sites, the three components were inverted. Figure 8c shows the inversion results considering the actual observational network and the 3D plate interface introduced by Radiguet et al. (2016) (gray contours). Although solutions are degraded as we move from the simplest (Figure 8a) to the most realistic case (Figure 8c), it is remarkable how well the checkerboard slip pattern is reconstructed for all cases for a distance of up to ~ 200 km inland from the trench in the region around the GGap. Furthermore, the slip is well recovered offshore all the way up to the trench in the subduction segment where the ocean bottom instruments are located. In contrast, in the segment further southeast where no instruments of this kind are present, the slip is poorly

resolved beyond 20 km from the coast (Figure 8c). As a reference, the black contour depicts the 5 cm slip contour determined by Cavalier et al. (2013) for the 2006 SSE in Guerrero. Within that region, the checkerboard is reasonably well resolved in all cases.

To illustrate the benefit of the improved geodetic network for imaging SSEs, we inverted a Gaussian slip distribution (target model shown in Figure 8d) excluding (Figures 8e) and including (Figures 8f) the geodetic instruments provided by the government of Japan. The target model was chosen to resemble the slip distribution determined by Cavalier et al. (2013) for the 2006 SSE (i.e. most of the slip is embedded within the black contour). The tests clearly show that the new observational network substantially improves the slip reconstruction not only between 20 and 40 km depth, but also below the coast and the adjacent offshore region, where we find a significant overestimation of the slip in the absence of marine stations and a dense GPS array (Figure 8e). This region is of especial interest because we don't know whether offshore slow slip plays a major role during the seismic cycle. In contrast, even with no model regularization for the inversion, the slip is remarkably well resolved everywhere using the complete geodetic network (compare Figures 8f and 8d).

4. Conclusions and Perspectives

Thanks to a major collaborative effort between Mexican and Japanese scientists, we have instrumented the Guerrero seismic gap and neighboring regions with the first seismo-geodetic amphibious network in Mexico and Central America. This gap represents the largest natural threat to large populated areas such as Mexico City, with more than 22

million people, which may experience ground motions up to three times stronger than those felt during the disastrous 1985 Michoacan earthquake if the gap breaks in a similar or larger event. In that scenario, important coastal population centers such as Acapulco and Ixtapa-Zihuatanejo, among others, could also experience overwhelming ground shakings and tsunamis.

The observational network will produce unprecedented data in the region, which is expected to deepen our understanding of the subduction process and to provide more reliable estimates of the seismic and tsunami hazards along the Pacific coast of Mexico. To this purpose, participating researchers of the binational project are developing sophisticated physics-based models to simulate hypothetical scenario earthquakes in the GGap and the associated tsunamis with realistic inundations. These models are being constrained by observations from the observational network that, as shown in this paper, will benefit from high-resolution analyses of the crustal structure and the seismic coupling in the plate interface. Furthermore, risk management and educational experts from both countries are quantifying the vulnerability of coastal populations, and developing risk-mitigation guidelines along with local authorities of civil protection and school-teachers that are being implemented in this moment. As the project progresses in the next few years, detailed hazard assessments along the coast will be delivered to these experts for raising awareness and designing end-to-end risk mitigation recommendations in highly exposed localities.

Acknowledgments

The seismo-geodetic amphibious network and the associated binational research project is being funded by (1) the Japanese government through program “Science and Technology Research Partnership for Sustainable Development” (SATREPS) via the “Japan International Cooperation Agency” (JICA) and the “Japan Science and Technology Agency” (JST), and through the Universities of Kyoto (U of K) and Tokyo with grants number 15543611 and MEXT KAKANHI number 16H02219, respectively; and (2) the Mexican government through the “Universidad Nacional Autónoma de México” (UNAM) through grants numbers IN113814, IN111316, IG100617, IN115613 and IN107116, its “Coordinación de la Investigación Científica” (CTIC and COPO) with research vessel time, its central administration through importation fees, and its “Servicio Sismológico Nacional” (SSN); the “Consejo Nacional de Ciencia y Tecnología” (CONACyT) through grants numbers 268119, 273832 and 255308; the Mexican ministry of foreign affairs through the “Agencia Mexicana de Cooperación Internacional para el Desarrollo” (AMEXCID); and the “Centro Nacional de Prevención de Desastres” (CENAPRED). We specially thank the outstanding work of Arika Nagata, Kumiko Ogura, Vanessa Ayala, Liliana Córdova, Lorena García and José Antonio Santiago, as well as all the administrative staff from the U of K, UNAM, JICA, JST, AMEXCID, and CONACyT that made all this possible; and to the “Secretaría de Protección Civil del Estado de Guerrero” and the “Secretaría de Marina” (SEMAR) for their unconditional support.

References

Anderson, J.G., Bodin, P., Brune, J.N., Prince, J., Singh, S.K., Quaas, R. and Onate, M. (1986) Strong ground motion from the Michoacan, Mexico earthquake. *Science*, 233, 1043–1049.

Bensen, G. D., M. H. Ritzwoller, M. P. Barmin, A. L. Levshin, F. Lin, M. P. Moschetti, N. M. Shapiro, and Y. Yang (2007), Processing seismic ambient noise data to obtain reliable broad band surface wave dispersion measurements, *Geophys.J.Int.*, 169, 1239–1260, doi:10.1111/j.1365-246X.2007.03374.x.

Bartlow, N. M., N. M. Bartlow, S. Miyazaki, S. Miyazaki, A. M. Bradley, A. M. Bradley, P. Segall, and P. Segall (2011), Space-time correlation of slip and tremor during the 2009 Cascadia slow slip event, *Geophys. Res. Lett.*, 38, L18309, doi:10.1029/2011GL048714.

Calò, M., L. Parisi, D. Luzio (2013), Lithospheric P and S wave velocity models of the Sicilian area using WAM tomography: procedure and assessments. *Geophysical Journal International*. doi: 10.1093/gji/ggt252.

Cavalié, O., Pathier, E., Radiguet, M., Vergnolle, M., Cotte, N., Walpersdorf, A., Kostoglodov, V., Cotton, F., 2013. Slow slip event in the Mexican subduction zone: evidence of shallower slip in the Guerrero seismic gap for the 2006 event re-vealed by the joint inversion of InSAR and GPS data. *Earth Planet. Sci. Lett.* 367, 52–60. <http://dx.doi.org/10.1016/j.epsl.2013.02.020>.

Cotte, N., A. Walpersdorf, V. Kostoglodov, M. Vergnolle, J. Santiago, I. Manighetti, and M. Campillo (2009), Anticipating the next large silent earthquake in Mexico, *Eos Trans. AGU*, 90(21), 181–182.

Cruz-Atienza, V. M., A. Husker, D. Legrand, E. Caballero, and V. Kostoglodov (2015), Nonvolcanic tremor locations and mechanisms in Guerrero, Mexico, from energy-based and particle motion polarization analysis, *J. Geophys. Res. Solid Earth*, 120, 275–289, doi:10.1002/2014JB011389.

Chiarabba, C., and M. Moretti (2006), An insight into the unrest phenomena at the Campi Flegrei caldera from Vp and Vp/Vs tomography, *Terra Nova*, 18(6), 373–379.

Duke, C. M. and David J. Leeds Soil conditions and damage in the Mexico earthquake of July 28, 1957 *Bulletin of the Seismological Society of America* April 1959 49(2):179-191.

Frank, W. B., N. M. Shapiro, A. L. Husker, V. Kostoglodov, A. Romanenko, and M. Campillo (2014), Using systematically characterized low-frequency earthquakes as a fault probe in Guerrero, Mexico, *J. Geophys. Res. Solid Earth*, 119, doi:10.1002/2014JB011457.

Hirose, H., and K. Obara (2010), Recurrence behavior of short-term slow slip and correlated nonvolcanic tremor episodes in western Shikoku, southwest Japan, *J. Geophys. Res.*, 115, B00A21, doi:10.1029/2008JB006050.

Husker, A. L., V. Kostoglodov, V. M. Cruz-Atienza, D. Legrand, N. M. Shapiro, J. S. Payero, M. Campillo, and E. Huesca-Pérez (2012), Temporal variations of non-volcanic tremor (NVT) locations in the Mexican subduction zone: Finding the NVT sweet spot, *Geochem. Geophys. Geosyst.*, 13, Q03011, doi:10.1029/2011GC003916.

Iglesias, A., R. W. Clayton, X. Pérez-Campos, S. K. Singh, J. F. Pacheco, D. García, and C. Valdés-González (2010), S wave velocity structure below central Mexico using high-resolution surface wave tomography, *J. Geophys. Res.*, 115, B06307, doi:10.1029/2009JB006332.

Ito, Y., Hino, R., Suzuki, S., and Kaneda, Y. (2015). Episodic tremor and slip near the Japan Trench prior to the 2011 Tohoku-Oki earthquake. *Geophysical Research Letters*, 42, 1725–1731. doi:10.1002/2014GL062986.

Kostoglodov, V. and J. F. Pacheco (1999) Cien Años de Sismicidad en Mexico. Poster. Instituto de Geofísica, Universidad Nacional Autónoma de México.

Kostoglodov, V., S. Singh, J. Santiago, S. Franco, K. Larson, A. Lowry, and R. Bilham (2003), A large silent earthquake in the Guerrero seismic gap, Mexico, *Geophys. Res. Lett.*, 30(15), 1807, doi:10.1029/2003GL017219.

Kostoglodov, V., A. L. Husker, N. M. Shapiro, J. S. Payero, M. Campillo, N. Cotte, and R. W. Clayton (2010), The 2006 slow slip event and nonvolcanic tremor in the Mexican subduction zone, *Geophys. Res. Lett.*, 37, L24301, doi:10.1029/2010GL045424.

Lay, T., H. Kanamori, C. J. Ammon, K. D. Koper, A. R. Hutko, L. Ye, H. Yue, and T. M. Rushing (2012), Depth-varying rupture properties of subduction zone megathrust faults, *J. Geophys. Res.*, 117, B04311, doi:10.1029/2011JB009133.

Maury, J., S. Ide, V. M. Cruz-Atienza, V. Kostoglodov, G. González-Molina, and X. Pérez-Campos (2016), Comparative study of tectonic tremor locations: Characterization of slow earthquakes in Guerrero, Mexico, *J. Geophys. Res. Solid Earth*, 121, 5136–5151, doi:10.1002/2016JB013027.

Núñez-Cornú, F. J., M. Ortiz and J. J. Sánchez. The Great 1787 Mexican Tsunami. (2008). *Natural Hazards*. V. 47:569-576. DOI 10.1007/s11069-008-9239-1. (ISSN0921-030X; 1573-0840).

Payero, J. S., V. Kostoglodov, N. Shapiro, T. Mikumo, A. Iglesias, X. Pérez-Campos, and R. W. Clayton (2008), Nonvolcanic tremor observed in the Mexican subduction zone, *Geophys. Res. Lett.*, 35, L07305, doi:10.1029/2007GL032877.

Plessix, R. E. (2006), A review of the adjoint-state method for computing the gradient of a functional with geophysical applications, *Geophysical Journal International*, 167(2), 495–503.

Radiguet, M., F. Cotton, M. Vergnolle, M. Campillo, A. Walpersdorf, N. Cotte, and V. Kostoglodov (2012), Slow slip events and strain accumulation in the Guerrero gap, Mexico, *J. Geophys. Res.*, 117, B04305, doi:10.1029/2011JB008801.

Radiguet, M., H. Perfettini, N. Cotte, A. Gualandi, B. Valette, V. Kostoglodov, T. Lhomme, A. Walpersdorf, E. Cabral Cano, and M. Campillo (2016). Triggering of the 2014 Mw7.3 Papanao earthquake by a slow slip event in Guerrero, Mexico, *Nature Geoscience*, 9 (11), 829-833. doi:10.1038/ngeo2817.

Rawlinson, N. and M. Sambridge (2005). The fast marching method: An effective tool for tomographic imaging and tracking multiple phases in complex layered media, *Explor. Geophys.*, 36, 341-350.

Singh, S. K., L. Astiz and J. Havskov (1981). Seismic gaps and recurrence periods of large earthquakes along the Mexican subduction zone: A reexamination. *Bull. Seismol. Soc. Am.* 71, 827-843.

Singh, S. K., J. M. Espindola, J. Yamamoto and J. Havskov (1982). Seismic potential of Acapulco-San Marcos region along the Mexican subduction zone. *Geophys. Res. Lett.*, 9, 633-636.

Spica Z., Cruz-Atienza V. M., Reyes-Alfaro G., Legrand D., Iglesias-Mendoza A. (2014) Crustal imaging of western Michoacán and the Jalisco block, Mexico, from ambient seismic noise. *J Volcanol Geotherm Res* 289: 1–9. doi:10.1016/j.jvolgeores.2014. 11.005

Spiess, F. N., 1980. Acoustic techniques for marine geodesy, *Mar. Geod*, 4, 13–27.

Suárez, G. and P. Albini (2009), Evidence for great tsunamigenic earthquakes (M 8.6) along the Mexican subduction zone, *BSSA* 99(2A), 892–896, doi:10.1785/ 0120080201.

Tarantola, A., 1984. Inversion of seismic reflection data in the acoustic approximation, *Geophysics*, 49(8), 1259–1266.

Toomey, D.R. & Foulger, G.R., (1989), Tomography inversion of local earthquake data from the Hengill: Grensdalur central volcano complex, Iceland, *J. geophys. Res.*, 94, 17 497–17 510.

Toomey, D.R., R.M. Allen, A.H. Barclay, S.W. Bell, P.D. Bromirski, R.L. Carlson, X. Chen, J.A. Collins, R.P. Dziak, B. Evers, D.W. Forsyth, P. Gerstoft, E.E.E. Hooft, D. Livelybrooks, J.A. Lodewyk, D.S. Luther, J.J. McGuire, S.Y. Schwartz, M. Tolstoy, A.M. Tréhu, M. Weirathmueller, and W.S.D. Wilcock. 2014. The Cascadia Initiative: A sea change in seismological studies of subduction zones. *Oceanography* 27(2):138–150.

Udías, A., Madariaga, R., and Buforn, E. (2014). Source mechanisms of earthquakes: Theory and practice. Cambridge University Press. doi:10.1017/CBO9781139628792.

UNAM Seismology Group (2015). Papanoa, Mexico earthquake of 18 April 2014 (Mw 7.3). *Geofis. Int.* 54, 363-386.

Villafuerte, C., and V. M. Cruz-Atienza (2017), Insights into the causal relationship between slow slip and tectonic tremor in Guerrero, Mexico, *J. Geophys. Res. Solid Earth*, 122, doi:10.1002/2017JB014037.

Yamashita, Y., Yakiwara, H., Asano, Y., Shimizu, H., Uchida, K., Hirano, S., ... (2015). Migrating tremor off southern Kyushu as evidence for slow slip of a shallow subduction interface. *Science*, 348(6235), 676–679. doi:10.1126/science.aaa4242.

Zhang, H. and Thurber, C.H., 2003. Double-difference tomography: the method and its application to the Hayward fault, California, *Bull. seism. Soc. Am.*, 93, 1175–1189.

	Onshore	Offshore
Seismic	<p>14 seismological stations consisting of:</p> <ul style="list-style-type: none"> • 1 Kinematics STS-2.5 sensor with Quanterra Q330S digitizer. • 6 Reftek 151B-120 sensors with 6 Reftek 130-01 digitizers. • 5 Guralp CMG-40T and 2 Reftek 151-60 sensors with 7 Reftek 130-01 digitizers. 	<p>7 ocean bottom seismometers (OBS) consisting of:</p> <ul style="list-style-type: none"> • 7 Katsujima 1-Hz 3D sensors with HDDR-5 digitizer, and Tokyo Sokushin 1-Hz 3D digitizer with TOBS-24N.
Geodetic	<p>33 GPS stations consisting of:</p> <ul style="list-style-type: none"> • 11 Zephyr 2 and 3 geodetic antennas, and Trimble NetR9 receivers. • 22 Leica AT504 and Trimble Zephyr 2 geodetic antennas, and Trimble NetR9, Leica GRX1200, GRX1200 receivers. 	<p>7 ocean bottom pressure gages (OBP) consisting of:</p> <ul style="list-style-type: none"> • 4 Sonardyne FETCH with Paroscientific pressure sensor (3000 and 6000 m). • 3 OBPs Paroscientific Inc., 8B4000-2-005, with data logger, Hakusan LS-9150. <p>2 GPS-acoustic stations (GPS-A) consisting of:</p> <ul style="list-style-type: none"> • 4 Sonardyne FETCH without pressure sensor (3000 and 6000 m).

Table 1 Technical specifications of the equipment composing the seismo-geodetic amphibious network in the GGap provided by the Mexico-Japan collaborative project.

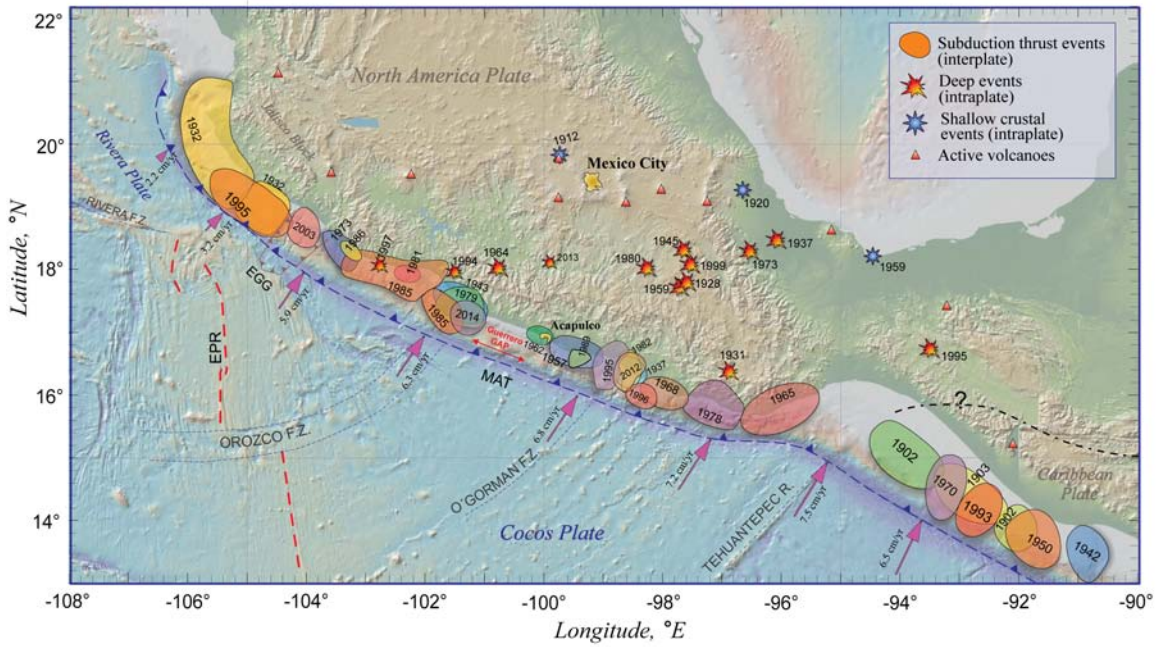


Figure 1 Map showing the tectonic setting of central Mexico and the main rupture areas and epicenters of large earthquakes since year 1900 (modified from Kostoglodov and Pacheco, 1999).

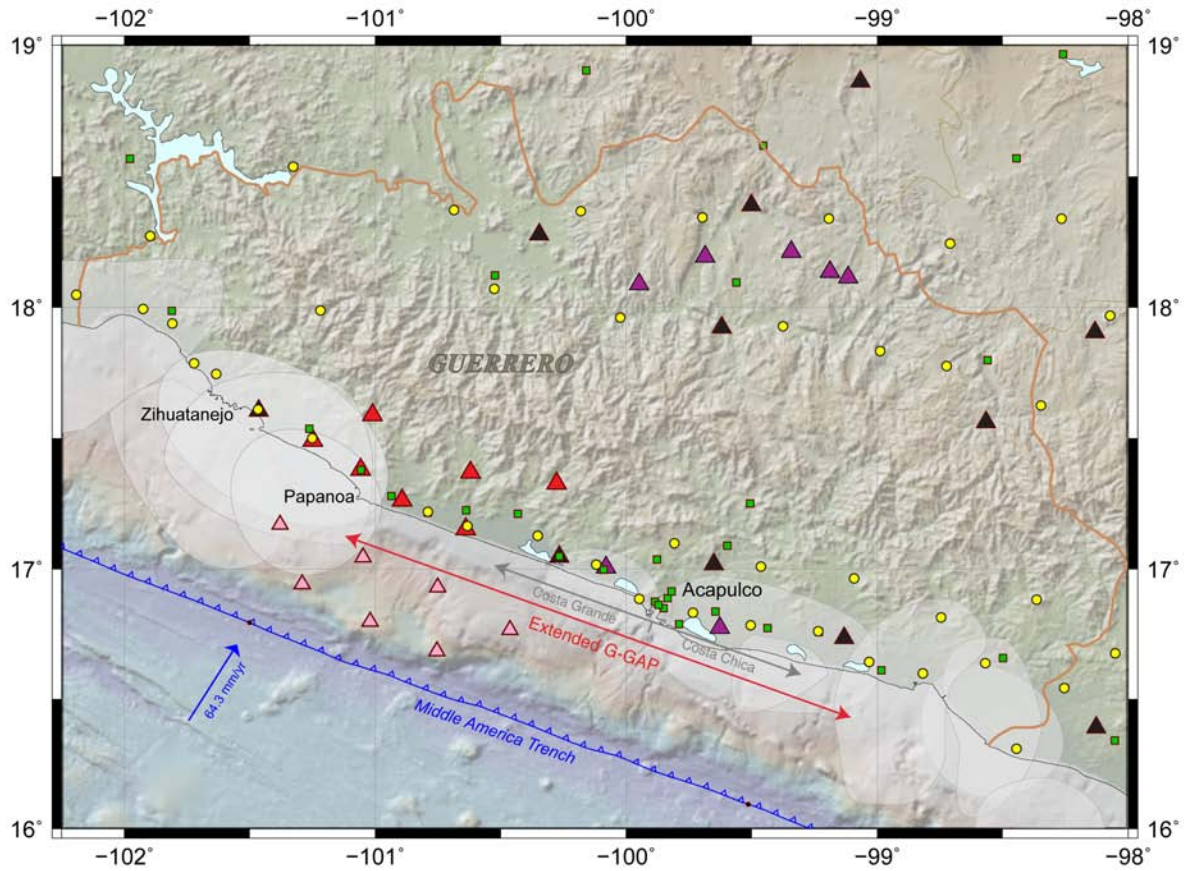


Figure 2 Seismological amphibious network in the GGap and nearby regions. Broadband seismic stations provided by Japan (red), broadband seismic stations from Mexico-UNAM (purple), broadband and strong motion from the SSN-UNAM (black), OBSs from Japan (pink), strong motion stations from the Institute of Engineering-UNAM (green) and strong motion stations from CIRES-SASMEX (yellow). Shading areas represent the approximate rupture areas from large earthquakes since 1911 (modified from Kostoglodov and Pacheco, 1999).

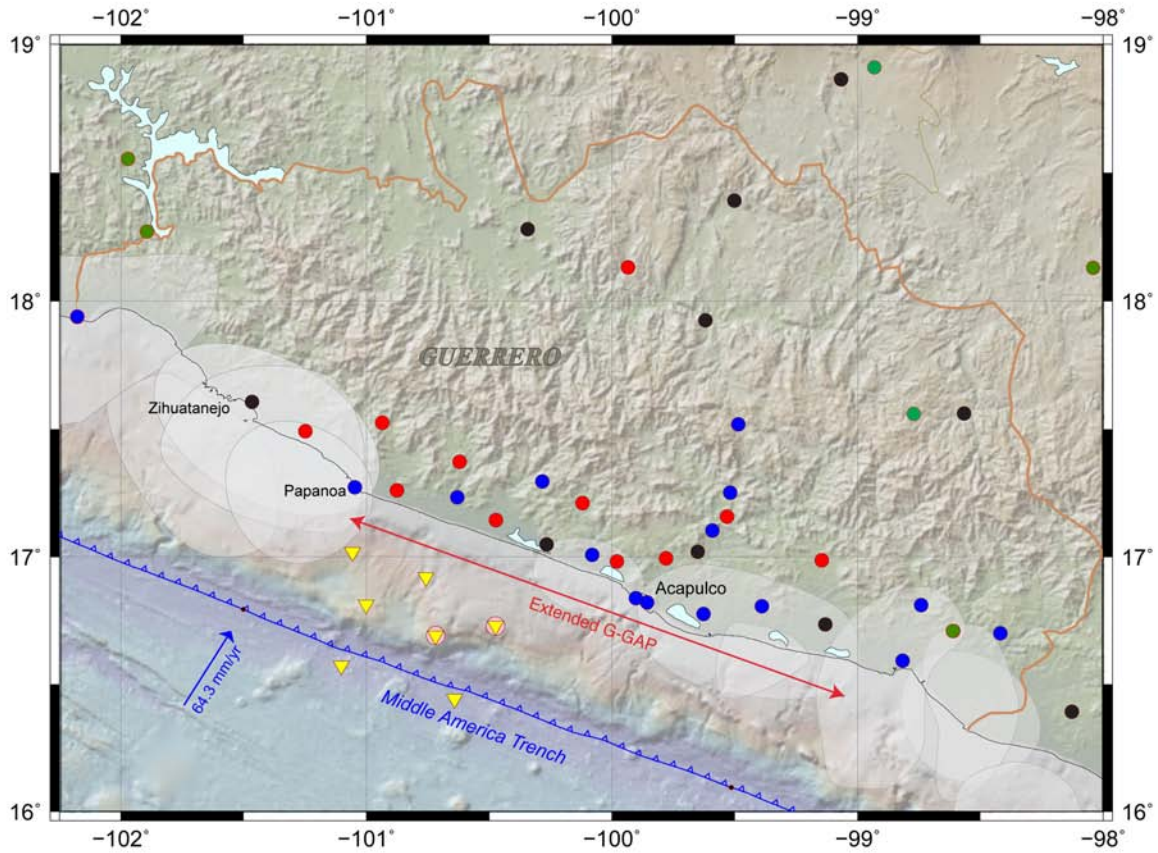


Figure 3 Geodetic amphibious network in the GGap and nearby regions. GPS stations from Japan (red), GPS stations from Mexico-UNAM (blue), GPS stations from the SSN-UNAM (black), GPS stations from the TlalocNet Mexico-UNAM (green), OBPs stations from Japan-Mexico (yellow) and GPS-Acoustic arrays from Japan-Mexico (pink circles). Shading areas represent the approximate rupture areas from large earthquakes since 1911 (modified from Kostoglodov and Pacheco, 1999).



Figure 4 Cartoon illustrating the ocean bottom instruments deployed in the GGap, which consists of 7 OBSs, 7 OBPs and 2 GPS-A sites (see Table 1 for details). In the surface we illustrate both the R/V El Puma and the wave glider used for the GPS-A measurements.



Figure 5 Most of participants of the workshop held in Nara, Japan, in the framework of the 2016-2021 Mexico-Japan collaborative project. During this meeting, more than 50 scientists (26 from Mexico) of about 12 different research institutions from both countries discussed in July 26-28, 2017, the advances and perspectives of the project.

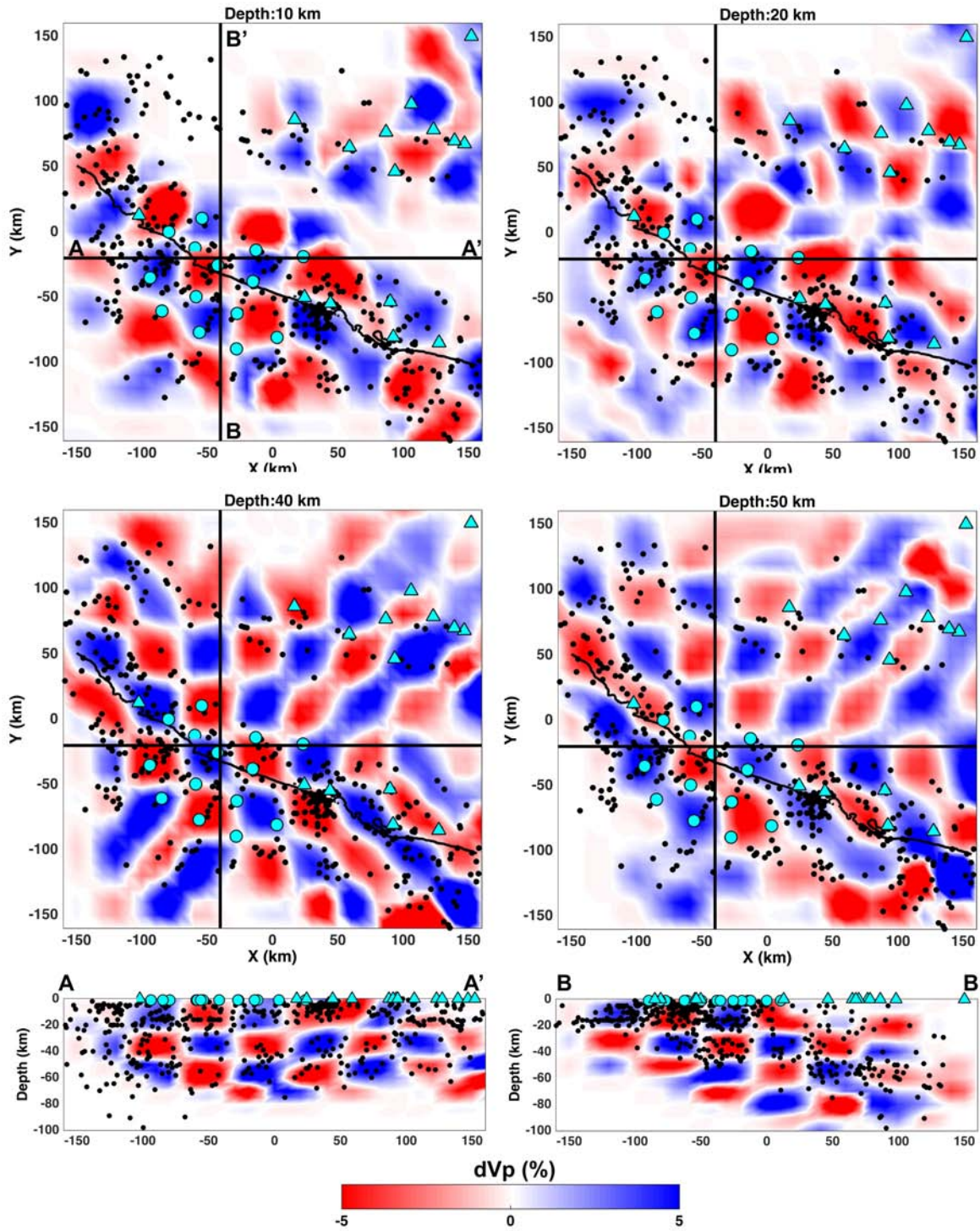


Figure 6 Checkerboard resolution test for double-difference travel time tomography. The checkerboard velocity cells are 20 x 20 km length horizontally and 10 km in depth.

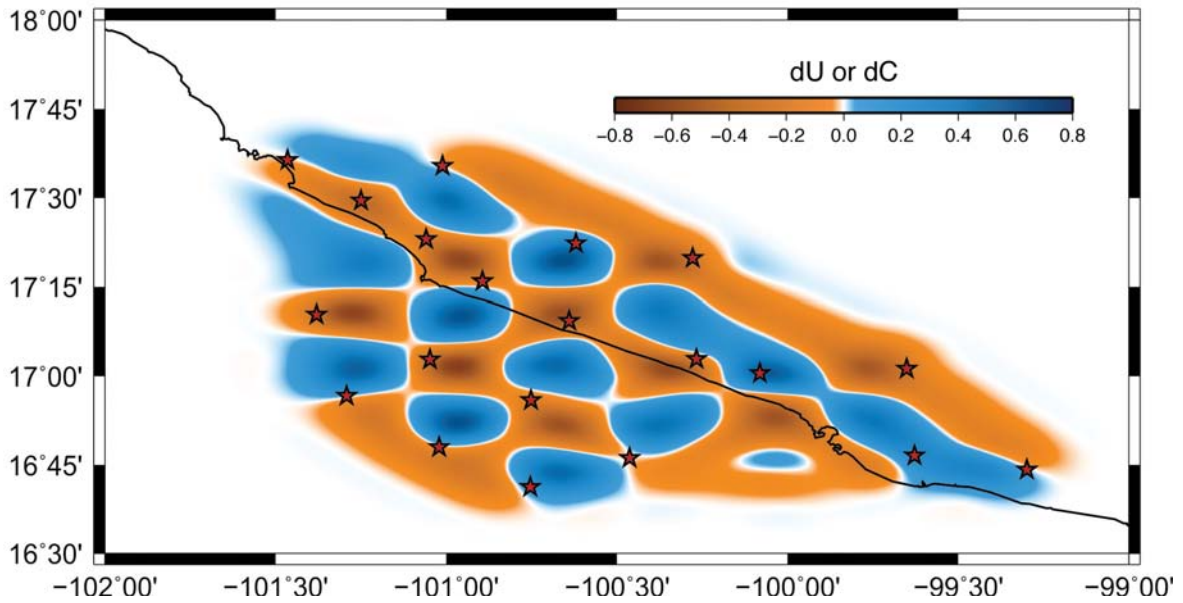


Figure 7 Checkerboard resolution test assuming that it is possible to obtain travel times (corresponding to phase, C, or group, U, velocities) between all pairs of stations from the cross correlation of seismic noise. The checkerboard velocity cells are 0.1° (~ 11 km) per side.

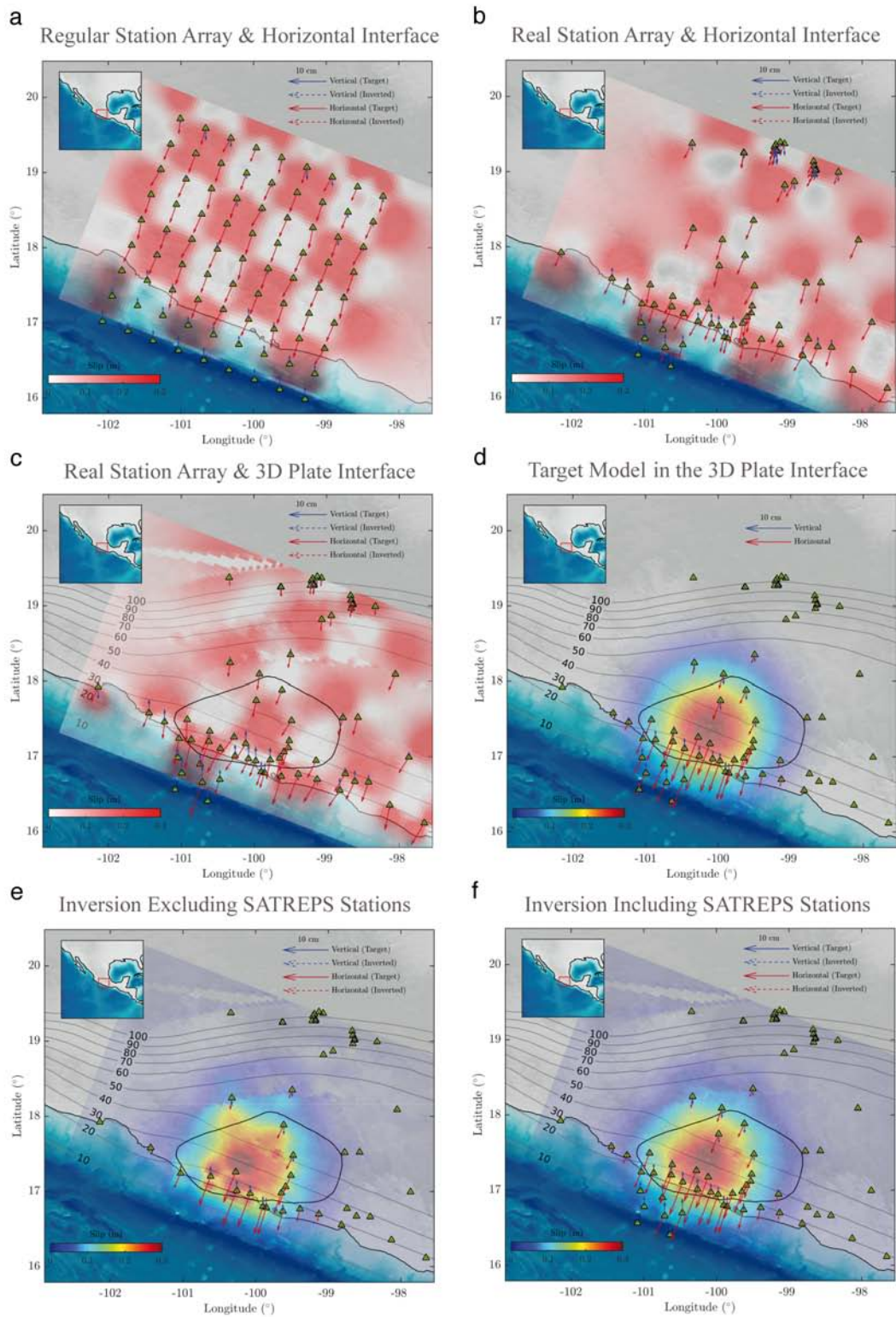


Figure 8 Synthetic inversion tests using a recently developed adjoint inverse method for imaging slow slip events and the seismic coupling in the plate interface. Panels a-c show

results from checkerboard tests with different model setups as described in the panels' titles. Panels e and f show the inversion results excluding and including the geodetic stations provided by the Japanese government, respectively, for the Gaussian slip distribution shown in panel d. The black contour depicts the 5 cm slip contour determined by Cavalier et al. (2013) for the 2006 SSE in Guerrero.